Effects of Notch Acuity and Side Grooving on Fracture Toughness

Test program is aimed at developing a low cost, small specimen test more reliable than present impact and slow bend tests

BY E. SMITH AND B. M. PATCHETT

Published in Two Parts

Part II — Slow Bend

ABSTRACT. Slow bend tests were carried out on plain and side grooved Charpy-sized specimens of Hyplus 29 steel containing either Charpy V or 0.15 mm slit notches and with a constant notched cross section of 80 mm^2. Increasing notch acuity had little influence on the lateral expansion (LE) for complete ductile fracture or on the fracture appearance transition temperature (FATT), but reduced the critical crack opening displacement (COD) and the critical LE for ductile crack initiation by about 10%, lowered the critical COD and LE in the brittle region by about 30%, and raised the COD and LE transition temperatures in the brittle region by about 20 C.

Side grooving considerably reduced the LE for complete failure and the LE and COD for crack initiation in the ductile region, but the effect decreased with decreasing temperature. Side grooving did not significantly influence either the FATT or the LE transition temperatures when the latter were plotted as percentages of the upper shelf value.

A technique for separating the initiation and propagation stages of fracture is described based upon measurements of LE made at the point of crack initiation and again after complete failure. In all specimen types the separation of the initiation and propagation stages of fracture occurred at the same temperature. This characteristic transition temperature, named the nil-arrest temperature (NAT), was compared with the nil-ductility transition temperature (NDT) determined from Pellini drop weight tests on full thickness material.

The results are compared with those obtained in an earlier program using impact loading and the practical implications of the results are discussed.

Introduction

In Part I (Ref. 1) it was shown that for impact loading an increase in notch acuity from a Charpy V to a 0.15 mm slit had no significant influence on the ductile fracture behavior or the fracture appearance transition temperature (FATT) of Hyplus 29 steel. In the brittle region, however, transition temperatures were raised by an average of 27 C and toughness parameters were reduced by up to 50%. Side grooving to depths of 1 mm and 2 mm considerably reduced energy absorption and lateral expansion (LE) in the ductile region but the effect decreased with decreasing temperature. Side grooving raised the FATT by 23-32 C, depending on the depth of side groove, and raised the energy absorption and LE transition temperatures by a similar amount when the values were plotted as percentages of the upper shelf. A specimen design incorporating a slit notch and 2 mm side grooves produced a 100% crystalline fracture at the NDT of the steel used.

This paper presents the results of tests on the same six specimen types used in Part I but using a slow strain rate.

Material

The material and specimen preperation was the same as that described in Part I (Ref. 1).

Procedure

The specimens were tested in an Instron machine using three point bending over a span of 40 mm at a cross head speed of 2×10^{-2} mm/s (5×10^{-2} in./min). Temperatures were monitored by Chromel-Alumel thermocouples capacitor discharge welded close to the top surface of the specimen. Temperatures down to -100 C were obtained by immersing the specimen in a mixture of Methanol and liquid nitrogen, and the recorded temperatures were accurate to within 2 C. For lower temperatures the specimen was surrounded by nitrogen vapor and the recorded temperatures were accurate to within 5 C.

(Part 1 of this article appeared in the June Research Supplement starting on page 169-s).

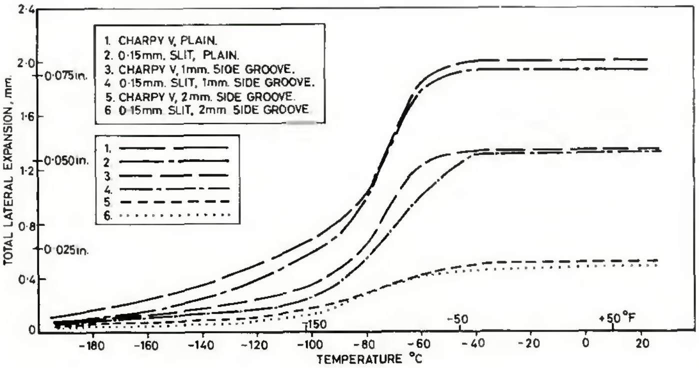

Fig. 1 — *Variation in total lateral expansion for failure with temperature*

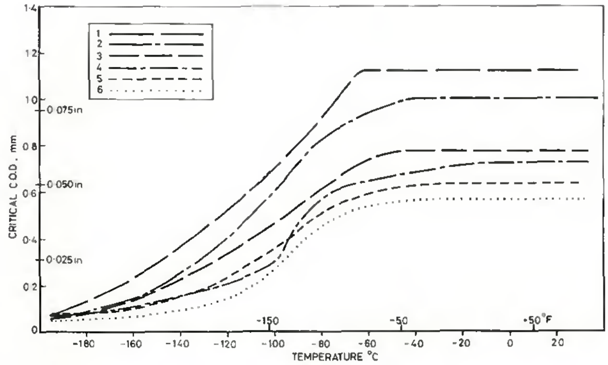

Fig. 3 — *Variation in critical crack opening displacement for crack initiation with temperature*

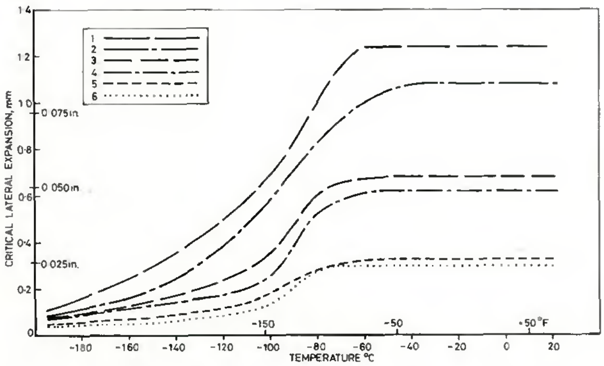

Fig. 2 — *Variation in critical lateral expansion for crack initiation with temperature*

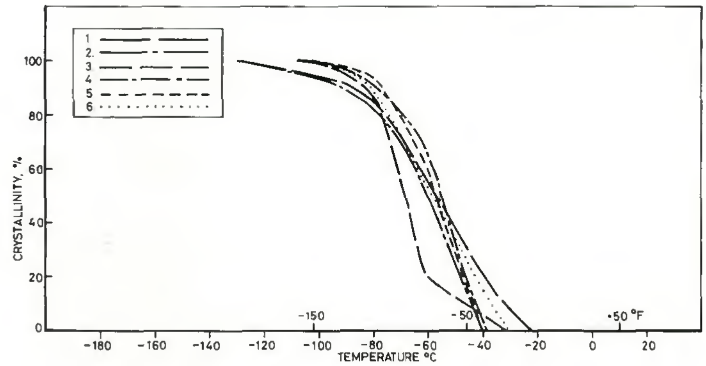

Fig. 4 — *Variation in fracture appearance with temperature*

Crack opening displacement (COD) was monitored during each test using a double cantilever beam made by fitting extension arms to a 12 mm (0.5 in.) Instron extensometer which was positioned between knife edges screwed onto the top surface of the specimen. The calibration range of this clip gage, however, precluded the measurement of the very large opening displacements obtained in the upper shelf region, although it was perfectly satisfactory at lower temperatures. The following technique was adopted, therefore, to measure these high values of COD and also to measure LE values at the onset of crack initiation and again after complete failure.

Prior to test the distance between the knife edges and the width of the specimen opposite the notch was measured using a traveling microscope. The specimen was then cooled to the desired test temperature and continuously loaded until a maximum load behavior was indicated by the first slight drop in load. The specimen was then unloaded and the distance between the knife edges and the width of the specimen measured to yield values for COD and LE at the onset of crack initiation. The specimen was then recooled to the test temperature and loaded until complete failure occurred. The LE was again measured to yield values for complete failure equivalent to those measured in the impact tests.

In a number of tests it was possible to measure the critical COD for crack initiation by both methods, i.e., from the clip gage reading ("on-load" value) and from the traveling microscope measurements ("off-load" value). The "off-load" values averaged 5% less than the "on-load" values, which is not considered to be significant. Wherever possible the "on-load" values are used.

For temperatures at which the specimens fractured under a rising load, the clip gage was able to monitor the COD up to the point of fracture. In such cases complete fracture occurred as soon as the crack initiated.

Full transitional behavior was determined for each of the six specimen types by testing a minimum of 36 specimens over the temperature range 20 C to −196 C.

Results

The variation in LE for complete failure, the LE and COD for crack initiation, and fracture appearance with temperature are shown in Figs. 1-4. The experimental points fell close to the curves but have been omitted for sake of clarity. As in the previous report the influence of the variables notch acuity and side grooving have been quantified by measuring shifts in transition temperature and by measuring changes in the various toughness parameters at fixed temperatures. In addition, the influence of strain rate is quantified in a similar manner by comparing the present results with the impact test results.

Influence of Notch Acuity on Transition Temperature

Figure 1 shows that increasing the notch acuity from a Charpy V-notch to a 0.15 mm slit has little influence on the LE for complete fracture in the ductile region, but at low temperatures there is a decrease in LE and an increase in transition temperature. Specific changes are shown in Table 1, which also includes average values from the impact tests. There is very close agreement between the changes in the LE and COD transition temperatures which results from the near linear relationship between these two parameters shown in Fig. 5. The increases in transition temperature are slightly less than shown by the impact tests but in both cases the only significant effect occurs in the brittle region, where the average Increase in slow bend (+20 C) is slightly less than that shown by the impact tests (+27 C). Notch acuity has no signif-

Table 1 — **Influence of Notch Acuity on Lateral Expansion and Crack Opening Displacement**

Side groove depth, mm	Toughness parameter	Increase in transition temperature deg C Ductile region	 Mid-transition region	 Brittle region
0	Lateral expansion	+1 (1.8 mm)	−1 (1.15 mm)	+18 (0.30 mm)
0	Crack opening displacement	—	+6 (0.80 mm)	+17 (0.30 mm)
1	Lateral expansion	+12(1.1 mm)	+6 (0.80 mm)	+21 (0.20 mm)
1	Crack opening displacement	—	+6 (0.60 mm)	+23 (0.20 mm)
2	Lateral expansion	0 (0.4 mm)	+2 (0.25 mm)	+18 (0.10 mm)
2	Crack opening displacement	—	+1 (0.50 mm)	+21 (0.10 mm)
	Average (Slow bend)	+4	+3	+20
	Average (Impact)	+4	+8	+27

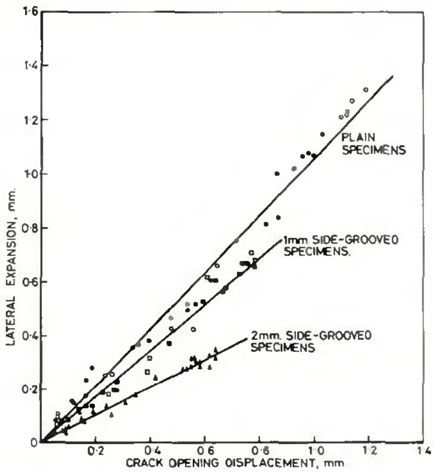

Fig. 5 — Relationship between crack opening displacement and lateral expansion

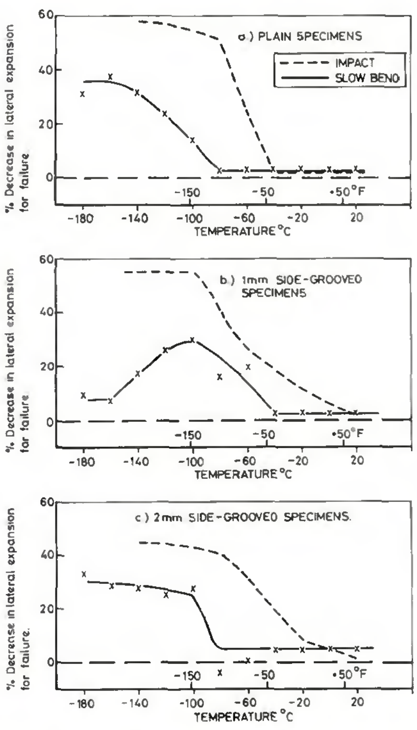

Fig. 6 — Influence of change in notch acuity from Charpy V to 0.15 mm slit on the lateral expansion for failure

icant influence on the FATT, *Fig.* 4; this is in accord with the impact test results.

Influence of Notch Acuity on Toughness Parameters

The influence of notch acuity on the LE for complete failure is shown in Fig. 6, which also includes the average changes observed in the impact tests. Although the general pattern shown by the slow bend and impact tests is similar, it is readily apparent that notch acuity becomes effective at a lower temperature in slow bend than in impact and that the decrease in LE observed at low temperatures is less marked in the slow bend tests. This is in accord with the smaller changes in transition temperature described in the previous section. With the plain specimens, notch acuity first becomes significant below −80 C and gives a maximum decrease in LE of 30 to 35% at temperatures below −140 C. With the 1 mm side grooved specimens notch acuity first becomes significant below −40 C and gives a maximum decrase of about 30% at −100 C. Below −100 C the effectiveness of notch acuity appears to decrease, although this is probably due to small inaccuracies in LE at these temperatures which can cause large errors in the plotted parameter. This may also account for the fact that with the 2 mm side grooved specimens notch acuity apparently first becomes significant below −80 C and gives a maximum decrease of about 30% at temperatures below −100 C, since the two points at *−60* and *−80* C are of dubious accuracy.

Notch acuity has a similar effect on the COD for crack initiation as shown in Fig. 7, although in this case there is a decrease of about 10% in the upper shelf values which is consistent with the results of other workers (Refs. 3 and 4).

Influence of Side Grooving on Transition Temperature

Figures 1-3 show that, as in the impact results, side grooving considerably reduces the toughness parameters especially at high temperatures and the effect decreases with decreasing temperature. However, unlike the impact tests where side grooving influenced the temperature at which the values fell from the upper shelf, in the slow bend tests all the specimen types fell from the upper shelf at about the same temperature. Side grooving also had no significant influence on the FATT in slow bend, Fig. 4, whereas the impact tests showed an increase of 23 C to 32 C due to side grooving. In addition, when the LE results are plotted as percentages of the upper shelf value little significant change in transition temperature is displayed by the 2 mm side grooved specimens, as shown in Fig. 8, although there is a slight increase for the 1 mm side grooved specimens.

Influence of Side Grooving on Toughness Parameters

The influence of side grooving on COD for crack initiation is shown in Fig. 9. Corresponding changes in energy absorption in the impact tests are included for comparison. Again a similar pattern is shown by the slow bend and impact tests, although the changes are less marked in slow bend. With both side groove depths the critical COD is reduced by a relatively constant amount outside the temperature range −80 to −160 C. Within this transition range the reduction in COD is more marked, by an additional 15%.

Influence of Strain Rate on Transition Temperature

The influence of increasing the strain rate from static to impact can be assessed by comparing the present results with those obtained in the impact tests. Comparison will be based on LE and fracture appearance since these methods of assessment were common to both.

The increases in the FATT brought about by increasing the strain rate from static to impact are shown in Table 2. With the plain specimens the average increase was quite small, about 8 C, while the 1 mm and 2 mm side grooved specimens showed much more substantial increases of 33 and 39 C respectively.

The influence of strain rate on the LE transition temperatures is shown in Table 3. More significant changes are shown compared with fracture appearance but again the changes shown by the plain specimens (average +24 C) is less than either the

1 mm side grooved (average +40 C) or the 2 mm side grooved (average +45 C) specimens.

Influence of Strain Rate on Toughness Parameters

The effect of increasing the strain rate from static to impact on the LE for complete failure is shown in Fig. 10. Some increase in LE is indicated at high temperatures but this is an anomalous effect due to the fact that in the slow bend tests the central loading point lost contact with the specimen after appreciable bending had occurred and thus the LE was not fully developed. In the impact tests, however, the machine pendulum bedded itself into the specimen and consequently the LE was fully developed.

With the plain specimens strain rate becomes effective below about −20 C and becomes fully effective below about −120 C when the decrease in toughness is about 60%. With the side grooved specimens strain rate becomes effective at a somewhat higher temperature, about 20 C, and reaches a maximum below about −60 C when the decrease in toughness is again about 60%.

Discussion

Notch acuity has been shown to influence the slow bend and impact tests in a similar manner, the only significant effect occurring at low temperatures when cleavage is the predominant mode of failure. The effect is less marked in slow bend where the average shift in transition temperature of 20 C contrasted with 27 C in impact while the corresponding changes in toughness parameters at low temperatures were 30-35% in slow bend and 45-60% in impact.

Similar changes were recorded in both the plain and side grooved specimens at each strain rate. The greater effectiveness of notch acuity in the impact tests suggests that the increased restraint associated with an increase in notch acuity is more readily maintained under high strain rate conditions due to the increase in yield stress under dynamic loading which promotes cleavage fracture. The only measurable effect of notch acuity in the ductile region was a 10% reduction in the upper shelf values of COD and LE for crack initiation associated with an increase in notch acuity in the slow bend tests. The conditions for crack initiation were not determined in the impact tests so it is not possible to say whether this effect would also be observed under impact loading.

Most published works on the influence of notch acuity on toughness (Refs. 3-8) have dealt with slow bend tests in a range of steels from C-Mn to low alloy quenched and tempered steels and have compared machined slits, similar to those used in the present work, with fatigue notches. Increases in transition temperature varied from marginal (Ref. 8) to 70 C (Ref. 6), although in most cases accurate predictions could not be made because of the large degree of scatter which characterized most of these tests. However a rise of 20-30 C in transition temperature is a reasonable average value and compares favorably with the changes observed in the present tests. This suggests that changing the notch acuity from a Charpy V-notch to a fatigue crack will raise the transition temperature by about 40-50 C. Other workers (Refs. 3-4) have reported a 10-20% drop in the upper shelf COD for ductile crack initiation when slit notches were replaced by fatigue notches, which suggests that a drop of 20-30% would be associated with the replacement of Charpy V-notches by fatigue notches.

Side grooving considerably reduced the toughness parameters in the upper shelf region in both slow bend and impact tests but became

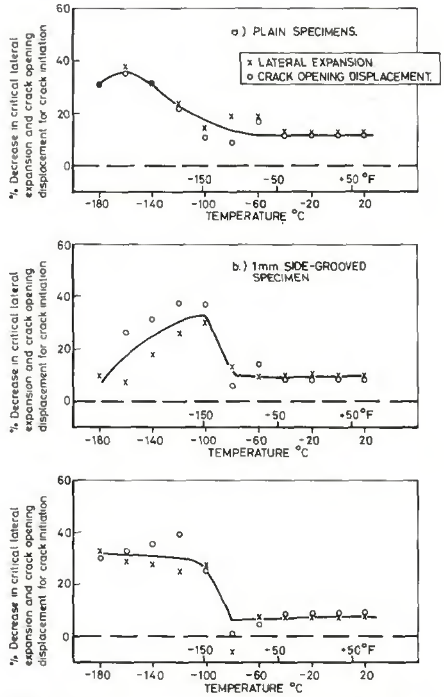

Fig. 7 — Influence of change in notch acuity from Charpy V to 0.15 mm slit on critical lateral expansion and crack opening displacement for crack initiation

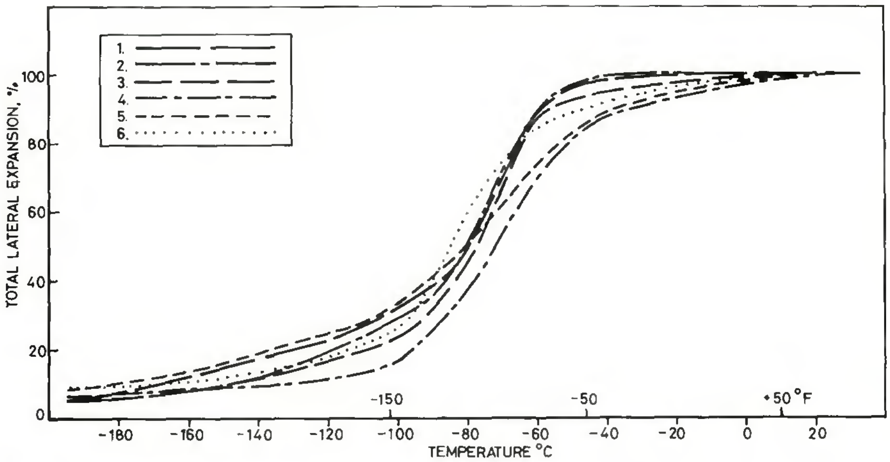

Fig. 8 — Variation in % lateral expansion with temperature

Table 2 — Influence of Increasing Strain Rate from Slow Bend to Impact on Fracture Appearance Transition Temperatures

Specimen type	Increase in fracture appearance transition, deg C		
	20% crystal-linity	50% crystal-linity	80% crystal-linity
Plain Charpy V-notch	+8	+6	0
Plain 0.15 mm slit notch	+16	+9	+7
Plain — average	+12	+7.5	+3.5
1 mm side grooved Charpy V-notch	+47	+38	+22
1 mm side grooved 0.15 mm slit notch	+40	+30	+23
1 mm side grooved — average	+43.5	+34	+22.5
2 mm side grooved Charpy V-notch	+41	+42	+33
2 mm side grooved 0.15 mm slit notch	+34	+46	+39
2 mm side grooved — average	+37.5	+44	+36

less effective with decreasing temperature. At both strain rates, however, the percentage reduction in toughness parameters was most pronounced in the mid-transition region and once again the changes were

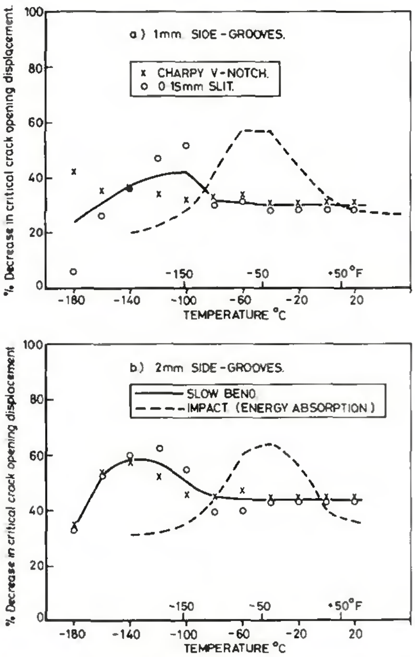

Fig. 9 — Influence of side grooving on critical crack opening displacement

more marked in the impact tests (60%) than in the slow bend tests (40-60%). One difference between the slow bend and impact tests was in the influence of side grooving on the FATT. In the impact tests this transition was raised by 23-32 C by side grooving while in the slow bend tests side grooving had no influence. With regard to crack propagation, an important distinction between the tests is that with impact loading the specimen is subject to an applied load after the crack initiates since the pendulum continues to supply energy to the specimen. If the initial speed of crack advance is greater than the cross head speed used in the slow bend tests, unloading will take place and, if the crack is not self propagating, arrest will occur. In the case of the impact tests on the plain specimens the propagation of the crack is inhibited by the low stressed regions at the specimen sides. Side grooving eliminates these low stressed regions and thereby ensures easier propagation. In the slow bend tests unloading occurs in both the plain and side grooved specimens and consequently both types show similar FATT.

Although side grooving was shown to reduce scatter substantially in the impact tests, no firm conclusions could be drawn from the slow bend tests since not enough tests were conducted at each individual temperature. The general impression was that neither notch acuity nor side grooving had any marked influence on scatter in the slow bend tests.

A valid comparison of the influence of strain rate on toughness behavior is limited to the LE and fracture appearance parameters, since these were the only measurements common to both the slow bend and the impact tests. High strain rate raises the transition temperatures of side grooved specimens more than plain specimens and it has a greater effect on the LE transition than on the FATT. With the plain specimens the average rise in the FATT was 8 C compared with 24 C for the LE transition, while in the side grooved specimens the rise in FATT of 33-38 C contrasted with a rise of 40-45 C in the LE transition. The greater rise in the LE transition temperature is probably due to the fact that it is strongly controlled by the conditions for crack initiation up to which point the relevant strain rates will be the applied ones. Once the crack initiates it will be subject to an enhanced strain rate which will be more marked in the slow bend tests. Consequently the difference in effective strain rates between the impact and slow bend tests will

Table 3 — Influence of Increasing Strain Rate from Slow Bend to Impact on Lateral Expansion Transition Temperatures

Specimen type	Increases in lateral expansion transition, deg C Ductile region	Mid-transition region	Brittle region
Plain Charpy V-notch	+21 (1.8 mm)	+ 7 (1.15 mm)	+37 (0.3 mm)
Plain 0.15 mm slit notch	+21 (1.8 mm)	+20 (1.15 mm)	+38 (0.3 mm)
Plain — average	+21	+13.5	+37.5
1 mm side grooved, Chapry V-notch	+49 (1.2 mm)	+43 (0.8 mm)	+36 (0.2 mm)
1 mm side grooved, 0.15 mm slit notch	+31 (1.2 mm)	+35 (0.8 mm)	+43 (0.2 mm)
1 mm side grooved — average	+40	+39	+39.5
2 mm side grooved, Charpy V-notch	+42 (0.45 mm)	+50 (0.35 mm)	+45 (0.1 mm)
2 mm side grooved, 0.15 mm slit notch	+37 (0.45 mm)	+55 (0.35 mm)	+40 (0.1 mm)
2 mm side grooved — average	+39.5	+52.5	+42.5

Table 4 — Data from Slow Bend and Impact Tests Used in Calculating Dynamic Crack Opening Displacement

Specimen type		Slow bend tests			Impact tests				
Notch type	Side groove	NAT temp. C	% Xal at NAT	COD at NAT, mm	Estimated NAT, C	Energy at NAT, ft lb	LE at NAT, mm	Estimated COD at NAT	Conversion factor, c
V	none	−80	85	0.92	−82	34	0.81	0.77	0.023
slit	none	−83	85	0.79	−78	17	0.50	0.47	0.028
V	1 mm	−82	90	0.59	−77	20	0.28	0.33	0.0165
slit	1 mm	−81	91	0.57	−60	19	0.26	0.30	0.016
V	2 mm	−80	94	0.51	−56	26	0.17	0.33	0.013
slit	2 mm	−81	90	0.50	−38	27	0.21	0.40	0.015

diminish, resulting in less effect on the propagation characteristics which largely control the FATT.

In the side grooved specimens the greater rise in transition temperature with increasing strain rate is possibly due to the fact that the distinction between crack propagation in the impact tests and crack propagation in the slow bend tests is more easily observed when the low stressed regions at the sides of the specimen are eliminated by side grooving.

In the slow bend tests the measurement of LE at the point of crack initiation and again after complete fracture enables the initiation and propagation characteristics of the steel to be assessed from a single test. Examples of the type of transition curve established for specimen types 1 and 6 are shown in Fig. 11. A characteristic transition temperature can be defined as the temperature at which the initiation and propagation curves separate. For convenience this will be described as the nil-arrest temperature, NAT. All specimens tested below the NAT fractured under a rising load and complete fracture occurred as soon as the crack initiated. Above the NAT the load-displacement diagram showed a maximum load behavior indicative of a non-self-propagating crack. The increasing values of LE for failure observed above the NAT reflects an increasing resistance to crack propagation, while the resistance to crack initiation does not increase to any great extent. It was observed that the NAT was the same for each of the six specimen types and was therefore not influenced by either notch acuity or side grooving but the toughness parameters (COD & LE) at the NAT were strongly influenced by these geometric factors.

The NAT observed in the slow bend tests is somewhat analogous to the nil-ductility transition temperature (NDT) obtained in the Pellini drop weight and explosion bulge tests. The measured value of the NDT was −40 C which compares with the NAT in the slow bend tests of about −80 C. The difference of 40 C between these two transition temperatures is similar to the difference in the LE transition temperatures between the slow bend and impact tests on the side grooved specimens. More work on other steels of different chemistry and mechanical properties is necessary to determine whether these relationships have any general significance.

The almost linear relationship between energy absorption and LE in the impact tests (Ref. 1, Fig. 4) and between COD and LE in the slow bend tests, Fig. 5, suggests that a similar relationship exists between energy absorption and COD which could be utilized to measure dynamic COD values. The departure from linearity between energy absorption and LE in the impact tests at energy absorption values above about 85 J (60 ft lb) is relatively unimportant to the present discussion since the main region of interest is the low energy absorption range.

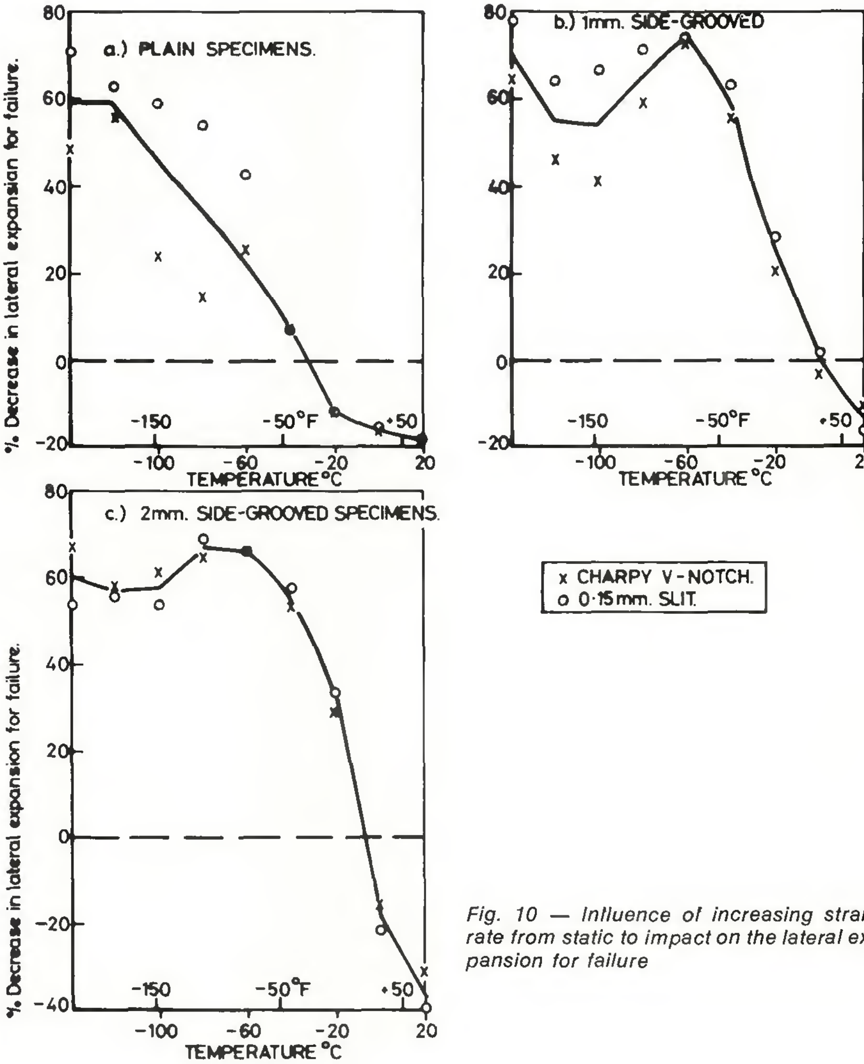

Fig. 10 — Influence of increasing strain rate from static to impact on the lateral expansion for failure

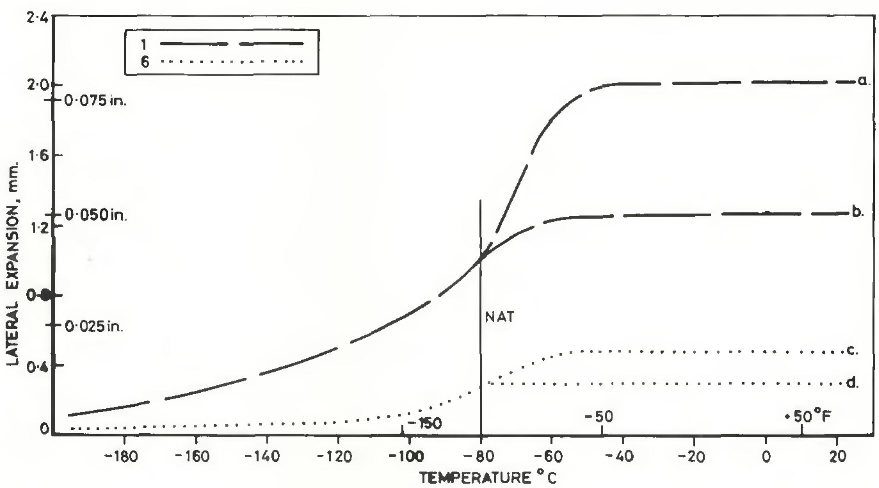

Fig. 11 — Variation in lateral expansion with temperature for specimen types 1 and 6; (a) lateral expansion for complete failure in specimen type 1; (b) lateral expansion for crack initiation in specimen type 1; (c) lateral expansion for complete failure in specimen type 6; (d) lateral expansion for crack initiation in specimen type 6

However, an important distinction has to be made between critical COD and energy absorption, since the former describes events occurring up to the onset of crack initiation while the latter describes events occurring up to the point of complete fracture. Figure 11 indicates that below the NAT temperature in the slow bend tests there is no resistance to crack propagation, so the solution to the problem becomes one of defining at which point on the impact transition curves the resistance to crack propagation also falls to zero. Once this is established the energy absorption values recorded below this temperature will be directly convertible into dynamic COD values for crack initiation. An indication of the temperature range over which this is possible can be suggested based on the following assumption.

In the slow bend tests the NAT temperature corresponded closely to the 85% crystallinity FATT for the plain specimens and the 90% crystallinity FATT for the side grooved specimens as shown in Table 4. This seems reasonable since the approach to zero crack propagation resistance will be associated with the attainment of predominantly cleavage fracture. Applying these relationships to the impact test results one can deduce the temperature at which the resistance to crack propagation falls to zero. These temperatures are included in Table 4 together with the energy absorption and LE values at this temperature. The dynamic COD values, obtained by conversion using the relationships shown in Fig. 5, are also included in the table. The conversion factors shown in the last column of the table can be used to calculate dynamic COD values on the basis of the following equation:

$$d = c\,E,\ \text{where}$$

d = dynamic COD in mm
E = energy absorption in ft lb
c = conversion factor (constant)

The equation is only applicable up to the energy absorption values shown in the table and, of course, is only applicable to the steel used in this investigation.

Some support for the validity of the values deduced in Table 4 can be derived by noting that the LE at the NAT in the slow bend tests closely approaches the upper shelf values for crack initiation, and that previous tests on a different steel (QT35) using a low energy blow technique (Ref. 9) indicated an upper shelf LE for crack initiation of 0.80 to 0.90 mm which compares favorably with the LE at the NAT of 0.81 mm quoted above for the same specimen geometry (plain Charpy V-notch) tested in impact.

The foregoing discussion indicates that fracture toughness values measured in the COD test are basically similar to those measured in the lower portion of the Charpy transition curve when identical specimens are used. The apparently large amount of scatter frequently associated with COD tests is therefore partly caused by the fact that these tests are simply an expanded version of the lower shelf region of a Charpy curve.

Conclusions

Slow bend tests on plain and side grooved specimens of Hyplus 29 steel containing Charpy V-notch and 0.15 mm slit notches have yielded the following information:

1. An increase in notch acuity does not affect the toughness parameters for complete ductile fracture or the FATT in either plain or side grooved specimens. However, it causes a drop of about 10% in the upper shelf COD and LE for crack initiation.
2. An increase in notch acuity raises the COD and LE transition temperatures in the brittle region by approximately 20 C (36 F) and reduces the low temperature toughness parameters by about 30% in both plain and side grooved specimens.
3. Side grooving considerably reduces COD and LE for crack initiation and LE for complete fracture in the ductile region but the effect decreases with decreasing temperature. The percentage decrease in COD for crack initiation is fairly constant at 30-40% outside the temperature range −80 C to −180 C (−112 F to −292 F) but rises to 40-60% within this range.
4. Side grooving does not influence the FATT or the LE transition when the latter is plotted as percentages of the upper shelf value.
5. An extension of the conventional COD test beyond the point of crack initiation enables the resistance of a material to both crack initiation and crack propagation to be assessed from a single test.

The following conclusions concerning the influence of strain rate on fracture toughness were derived from a comparison of the present results with those obtained in the impact tests (Ref. 1):

1. A change from slow bend to impact loading raises the transition temperature of the side grooved specimens more than the plain specimens. In all specimen types the LE transition temperature is raised more than the FATT.
2. At low temperatures the toughness parameters in impact are approximately 60% less in slow bend for all specimen types.

Practical Implications

The majority of fabrications which require quality control tests for fracture toughness are made from relatively low strength steels (e.g. the Hyplus 29 used in this work) which show significant fracture ductility in normal thicknesses. The aim of this program has been to develop a low cost small specimen test which is more reliable and realistic than present impact (Charpy) and slow bend (COD) tests. Although the results are confined to one steel composition and one thickness, the trends observed should be of general significance, and specific assessment of the effects of varying chemistry, strength and thickness should appreciably widen the range of application.

The specimen design changes assessed have eliminated the plane stress/plane strain fracture mixture usually observed in small specimens by a combination of high notch acuity and side grooving. Notch acuity has been shown to significantly affect "low temperature" fracture behavior, while side grooving has a more marked effect on "high temperature" fracture behavior. The combined result is a decrease in fracture toughness parameters at all temperatures, similar to the effects of increasing thickness and/or strength and also a very significant drop in the scatter caused by mixed mode fracture in the transition region.

Both these effects are significant for the test reliability and the accuracy of toughness parameters measured from specimens at less than full plate thickness.

In a welding situation, the specimen design changes have advantages for both heat-affected zone and weld metal assessment. Heat-affected zones vary in structure and strength over the width of the zone, and these variations cause testing problems as important as the changes in fracture toughness. For instance, changes in strength cause deformation strain to be transferred to weaker, often more ductile regions which may not have the lowest fracture toughness. Side grooving (more than notch acuity) assists in maintaining a fracture path, rather than allowing the fracture to follow the region of highest strain. Whether this is important for the overall welded joint performance is another question, but at least investigators will be able to unambiguously assess one structure at a time for its fracture properties, as long as a reasonably straight HAZ line can be produced.

In weld metals, where test scatter is very common, the suppression of mixed mode fracture will reduce scatter to some extent, but the structural variations due to solidification effects and multipass welding techniques will still be present and lead to some scatter in the results. Full thickness specimens are therefore necessary for procedural tests to assess the behavior of the complete joint (Ref. 9), but small scale tests should be adequate for subsequent quality control.

Multipass welds also suffer from a degradation in fracture toughness in the center region, especially in root runs (Ref. 10), but the significance of this on overall joint performance is not clear at present. Specimen design changes can minimize the disparity in values between central and surface specimens, but further full thickness testing will be necessary to determine which region dominates the fracture behavior. Such variations in toughness across the thickness are not restricted to multipass welds, since one of the authors has observed indentical behavior in single pass electroslag welds in mild and low alloy steels (Ref. 11).

In the impact tests, the results indicated that the No. 6 specimen design, with a slit notch and 2 mm side grooves, was probably the best design since it alone produced virtually 100% cleavage fracture (based on the FATT curve) at the NDT. This implies that the specimen simulates the full thickness fracture behavior of the 38 mm plate used, although the limit of the simulation is not known until thicker plate can be tested. It is also possible that thinner plates will be better assessed with shallower side grooves, but this also needs further tests on plates of between 19 to 38 mm.

In the slow bend tests, the choice of "best" specimen is more difficult. The experimental change in notch acuity had a fairly consistent effect on fracture behavior, but side grooving made a great difference in critical COD values compared to plain specimens, although all side groove depths were fairly closely grouped. The 1 mm side groove depth was shown to produce full width crack initiation, which is theoretically ideal. But the further reduction in COD values with the 2 mm side groove again raises the possibility that side groove depth may have to be a function of the full thickness to be simulated (or the degree of structural restraint required) with the 2 mm depth being used for greater thickness (high restraint conditions).

The authors feel that the emergence of the NAT as an apparent material property is important, since it may well be the testing equivalent of the NDT for slow bend conditions. Any specimen configuration may be used to determine it, and a plain sided specimen is probably best since measuring the LE is much easier with such specimens.

The parameter to be measured as an arbiter of fracture toughness is also of importance. The established methods of a given Charpy energy or crack displacement at a given temperature are not reliable enough, even with the improvement in scatter reduction achieved on this program. It is more important to know where on the fracture toughness transition curve the values are located, rather than their magnitude as such. This work indicates that the Pellini approach to crack propagation conditions, i.e., designing to a given temperature interval above the NDT, may also be applied to crack initiation conditions by designing to a temperature interval above the NAT to ensure that initiating cracks will not propagate.

References

1. Smith, E. and Patchett, B. M., "The Effects of Notch Acuity and Side Grooving on Fracture Toughness, Part 1 — Impact Loading," *Welding Journal,* Vol. 54 (6) June, 1975, Res. Suppl., pp 169-s to 177-s.

2. Jolley, G., Kilpatrick, L. M. and Main, R., "Effect of Notch Acuity on the Fracture Toughness of Three Low Alloy High Yield Strength Steels," *Welding Journal,* 52, (12). Dec. 1973, Res. Suppl., 543-s to 548-s.

3. Birkbeck, G. and Wraith, A. E., "Direct Surface Measurement of the Crack Opening Displacement of Mild Steel Charpy Specimens," *Proc. Int. Conf. on Fracture,* Paper 3, Brighton, 1969, 24 to 30.

4. Frederick, G. and Salkin, R. V., "Fracture Mechanics Assessment of Steel Plates to Brittle Fracture," *Symposium on Practical Application of Fracture Mechanics to Pressure Vessel Technology,* Institution of Mechanical Engineers 3-5 May, 1971, 136 to 147.

5. Elliot, D. and May, M. J., "The Assessment of Fracture Toughness of Low Strength Structural Steels Using General Yielding Fracture Mechanics," *B.I.S.R.A. Open Report,* MG/C/51/68, 1968.

6. Elliot, D. and May, M. J., "The Fracture Toughness of Two Low Strength Structural Steels," *B.I.S.R.A. Report,* MG/E/304/68, 1968.

7. Burdekin, F. M., "Initiation of Brittle Fracture in Structural Steels," *Welding Institute Report,* E/11/66, Abington Hall, Abington, Cambridge, England.

8. Smith, E., "A Study of the Charpy V-notch Impact Test," *Cranfield Institute of Technology Report,* Mat. No. 10, Cranfield, Bedford, England, 1973.

9. Dawes, M. G., "Fracture Control in High Yield Strength Weldments," *Welding Journal,* Vol. 53 (9) Sept. 1974, Res. Suppl., pp 369-s to 379-s.

10. Nicholson, S. and Rogers, P. F., "Controlling Weld Metal Toughness in Manual Metal Arc Welds," *International Conference on Welding in Offshore Constructions,* Paper 11, Newcastle-upon-Tyne. The Welding Institute, February, 1974.

11. Patchett, B. M., Unpublished work, Cranfield Institute of Technology.

Correction

The paper, "Investigation of Alloy 600 Welding Parameters," appearing on pages 113-s to 122-s of the April issue, should be revised to include the following alterations:

1. Page 115-s, Table 2: Current shown as 215 A should be 115 A.
2. Page 116-s, Table 4: Data for the 91 A current with the 90 mils arc gap for the T-4 reading should be 265 F instead of 500 F and the 91 A current with the 120 mils arc gap for the T-3 reading should be 500 F instead of 265 F.
3. Page 119-s, Fig. 13: The data on the graph should show 72 Btu/min instead of 56 Btu/min and 36 Btu/min instead of 28 Btu/min.
4. Page 120-s, Moving Arc: The first paragraph should read "Two moving arc calculations with an assumed heat input of 72 Btu/min and 36 Btu/min . . ." instead of "56 Btu/min and 28 Btu/min . . ."

Authors —

Abstracts for papers to be presented at the 57th Annual Meeting are due August 15, 1975 (see Form, page 395, May issue) — for Brazing and Soldering papers, deadline is September 15, 1975 (see Form, page 213, March issue).

Author's application forms may also be obtained by contacting T. P. Schoonmaker (general welding) or T. J. Olivera (brazing and soldering) at AWS, 2501 N.W. 7th St., Miami, Fla. 33125 — (305) 642-7090.

WRC Bulletin 201 December 1974

1. "The Submerged Arc Weld in HSLA Line Pipe — A State-of-the-Art Review"
by P. A. Tichauer

The submerged arc weld in HSLA line pipe is examined by briefly reviewing the metallurgy of high-strength low-alloy steels and then considering how the welding process affects this metallurgy. Particular emphasis is given to the influence of thermo-mechanical processing and to the role of micro-alloy additions as they relate to strength, grain size and toughness. The metallurgy of the weld is contrasted to that of the base plate, and some recent investigations are reviewed. The influence of consumable selection is considered, and some recommendations for further study are made.

2. "Experience in the Development and Welding of Large-Diameter Pipes"
by M. Civallero, C. Parrini and G. Salmoni

The production of X70 pipes up to 30 mm wall thickness with high base-material toughness has become necessary and possible today. In the choice of the most suitable type of steel, the mill and field weldability problems have been considered, as well as the weld-joint toughness requirements.

Of the experimental solutions, the best appears to be a control-rolled dispersoid steel, with extra-fine structure (mostly acicular type) with reduced pearlite and controlled inclusions. This steel, welded with the normal double-pass submerged arc techniques, allows one to achieve good toughness in the heat-affected zone, and to improve weldability compared to conventional steels. By further improving the type of flux on the basis of the theories developed, and by widening the knowledge of the effects of chemical composition (correlation between chemical composition, liquid-and-solid, austenite-to-ferrite transformation and final structures), it is believed possible to improve the low-temperature toughness up to the 10 kg/cm^2 level at temperatures down to -40 C, in wall thicknesses up to 30 mm.

3. "New Development in Weldability and Welding Technique for Arctic-Grade Line Pipe"
by E. Miyoshi, Y. Ito, H. Iwanaga and T. Yamura

In this study, low-temperature burst tests were performed on 48-in. diameter × 1-in. thick × 8-ft long line-pipe specimens of a 1% Ni steel recently developed and produced by controlled rolling. Notches twice the size of the largest allowable defect in API Std. 1104 were incorporated in the longitudinal weld seam. Test data were assessed by a COD approach. Two heat inputs were used in welding the specimens. A special GMA welding technique was developed for the lower heat input. It was found that the lower heat input was the best method of improving the fracture toughness of the weld.

4. "Technology of Wires and Electrodes for Welding High-Strength Pipe"
by J. Grosse-Wordemann

During the past few years, developments have led to steel grades with improved mechanical properties and reduced carbon content, compared to the previously known carbon-manganese grades. The new steels have improved weldability and API grades X60, X65 and X70 are already in use. The development of X80 is close to completion. This paper reviews the latest technology in developing suitable filler metals for welding these high-strength line-pipe steels.

5. "Preliminary Evaluation of Laser Welding of X-80 Arctic Pipeline Steel"
by E. M. Breinan and C. M. Banas

Single- and dual-pass laser welds were made in an alloy steel currently being evaluated for potential Arctic gas pipeline applications. The laser welds exhibited excellent overall mechanical properties and a Charpy shelf energy greater than 264 ft-lb, which is substantially above that of the base material. Dual-pass welds exhibited a ductile-to-brittle transition temperature below -60 F. Increased shelf energy was attributed to a reduction in the visible inclusion content of the fusion zone while transition temperature was shown to be strongly dependent upon fusion-zone grain size.

Paper (1) was prepared for the Subcommittee on Line-Pipe Steels of the Weldability (Metallurgical) Committee of the Welding Research Council. The other four papers were presented at a session sponsored by this subcommittee during the 1974 AWS Annual Meeting.